



HHS Public Access

Author manuscript

J Biomol NMR. Author manuscript; available in PMC 2021 September 01.

Published in final edited form as:

J Biomol NMR. 2020 September ; 74(8-9): 365–379. doi:10.1007/s10858-020-00331-z.

The precious Fluorine on the Ring: Fluorine NMR for biological systems

Andras Boeszoermyeni^{1,2,*}, Barbara Ogórek³, Akshay Jain¹, Haribabu Arthanari^{1,2}, Gerhard Wagner^{2,*}

¹Department of Cancer Biology, Dana-Farber Cancer Institute, 450 Brookline Avenue, Boston, MA 02215, USA

²Department of Biological Chemistry and Molecular Pharmacology, Harvard Medical School, 240 Longwood Avenue, Boston, MA 02115, USA

³Pulmonary and Critical Care Medicine, Department of Medicine, Brigham and Women's Hospital and Harvard Medical School, Boston, MA 02115, USA.

Abstract

The fluorine-19 nucleus was recognized early to harbor exceptional properties for NMR spectroscopy. With 100% natural abundance, a high gyromagnetic ratio (83% sensitivity compared to ¹H), a chemical shift that is extremely sensitive to its surroundings and near total absence in biological systems, it was destined to become a favored NMR probe, decorating small and large molecules. However, after early excitement, where uptake of fluorinated aromatic amino acids was explored in a series of animal studies, ¹⁹F-NMR lost popularity, especially in large molecular weight systems, due to chemical shift anisotropy (CSA) induced line broadening at high magnetic fields. Recently, two orthogonal approaches, i) CF₃ labeling and ii) aromatic ¹⁹F-¹³C labeling leveraging the TROSY (Transverse Relaxation Optimized Spectroscopy) effect have been successfully applied to study large biomolecular systems. In this perspective, we will discuss the fascinating early work with fluorinated aromatic amino acids, which reveals the enormous potential of these non-natural amino acids in biological NMR and the potential of ¹⁹F-NMR to characterize protein and nucleic acid structure, function and dynamics in the light of recent developments. Finally, we explore how fluorine NMR might be exploited to implement small molecule or fragment screens that resemble physiological conditions and discuss the opportunity to follow the fate of small molecules in living cells.

Terms of use and reuse: academic research for non-commercial purposes, see here for full terms. <https://www.springer.com/aam-terms-v1>

*Correspondence to: Andras_Boeszoermyeni@DFCI.harvard.edu or Gerhard_Wagner@hms.harvard.edu.

Author contributions: A.B., B.O and H.A. designed research; A.B., B.O and A.J. performed experiments; A.B. analyzed data., and A.B, H.A. and G.W. wrote the manuscript.

Publisher's Disclaimer: This Author Accepted Manuscript is a PDF file of an unedited peer-reviewed manuscript that has been accepted for publication but has not been copyedited or corrected. The official version of record that is published in the journal is kept up to date and so may therefore differ from this version.

Conflicts of interest/Competing interests: The authors declare no conflicts or competing financial interests.

Ethics approval: Not applicable, **Consent to participate:** Not applicable, **Consent for publication:** Not applicable

Code availability: Not applicable

Keywords

Fluorine NMR; TROSY; nucleic acids; proteins; drug discovery; 4-fluorophenylalanine

Introduction:

Due to an anisotropic distribution of electrons in the fluorine 2p orbitals, fluorine resonances are exquisitely sensitive to subtle differences in their van der Waals and electrostatic environments^{1,2}. However, this anisotropic electron distribution also gives rise to chemical shift anisotropy (CSA). The contribution of CSA to transverse relaxation increases rapidly with the magnetic field and the molecular weight of the system under investigation, limiting the applicability of fluorine NMR at high magnetic fields for biological systems. Two orthogonal approaches have been developed to address this problem. i) Site-specific labeling of cysteine residues with CF₃-carrying probes, such as trifluoroethanethiol³ and trifluoroacetanilide⁴. If direct interactions between the CF₃-group and the labeled protein can be avoided, then the rotation of the CF₃-group remains relatively free, mimicking a reduced molecular weight, even in big proteins. The presence of three magnetically equivalent fluorine atoms and the singlet appearance of the signal additionally contribute to the methods sensitivity. This approach has been applied to the study of G protein-coupled receptor (GPCR) dynamics³⁻⁶, to monitor conformational changes and to measure kinetic and thermodynamic parameters⁷⁻¹¹. An interesting variation of this strategy might be borrowed from NMR-based functional screening, where substrates are tagged with multiple magnetically equivalent CF₃-groups to enhance sensitivity¹². ii) The ¹⁹F-¹³C aromatic TROSY¹³ experiment, which selects for the slowly relaxing (Transverse Relaxation Optimized Spectroscopy) TROSY components of the fluorine and carbon resonances in an aromatic ¹⁹F-¹³C spin-pair. The TROSY effect works on the same principle as the previously reported ¹H-¹³C aromatic TROSY^{14,15}, but there is relatively better cancellation of the CSA induced relaxation in the aromatic carbon attached to ¹⁹F (¹³C_F) compared to the corresponding carbon attached to ¹H. This results in the dispersion of broadened fluorine signals into a second ¹³C-dimension with narrow linewidths and enables the investigation of large proteins and their interactions. For example, we exploited the ¹⁹F-¹³C TROSY to observe a weak (K_d: ~10 mM¹⁶) interaction of the 180-kDa α7 single-ring of the 20S proteasome core particle (CP) from *Thermoplasma acidophilum* with the antimalaria drug chloroquine (CQ) (Figure 1).

While the sensitivity of CF₃ labels is significantly better than that of fluorine substituted aromatic moieties, the ¹⁹F-¹³C aromatic TROSY approach allows for simultaneous labeling of all representatives of one type of aromatic amino acid across a protein, or nucleobase across a nucleic acid, which provides multiple probes to investigate the molecule of interest. Site-specific CF₃ labeling is generally restricted to proteins, although CF₃ methylated nucleobases represent an excellent and more versatile alternative for nucleic acids¹⁷, and the use of only one label. It also relies on the availability of a cysteine residue that can be targeted specifically. However, the most striking advantage of fluorine substituted aromatic amino acids comes from the fact that they are easily incorporated into proteins *in vivo*. Here, we will discuss fascinating early work with fluorine substituted aromatic amino acids and

nucleobases and potential applications of the ^{19}F - ^{13}C aromatic TROSY to monitor interactions and functions of biomolecules. Then, we will discuss the utility of CF_3 and aromatic fluorine substitutions on small molecules to monitor their interactions under physiological conditions. To limit the scope of this perspective, we will restrict the discussion to solution state NMR, despite the tremendous progress of fluorine NMR in the solid state with magic angle spinning beyond 25 kHz^{18,19}.

Fluorine substituted aromatic amino acids in mammals:

Studies in the late 1950s and early 1960s revealed that 4-fluorophenylalanine readily incorporates into the proteins of mammals^{20–23}. In a seminal publication, Westhead and Boyer showed 25% and 16% incorporation of 4-fluorophenyl-[3- ^{14}C]alanine fed to rabbits into aldolase and glyceraldehyde 3-phosphohate dehydrogenase, respectively²³. They inferred that assuming a roughly 2:1 phenylalanine to 4-fluorophenylalanine ratio in the diet fed to their rabbits, the high degree of 4-fluorophenylalanine incorporation suggests that rabbit tRNAs recognize the non-natural analogue with comparable efficiency to phenylalanine²³. Similar findings were also presented for 4-fluorophenylalanine uptake in proteins of mice²⁴, cats²⁵ and gerbils²⁶.

In later studies aimed at developing ^{18}F fluorinated amino acids as tracers for positron-emission tomography (PET), Weissman and Koe demonstrated that 4-fluorophenylalanine and 2-fluorophenylalanine showed low toxicity ($\text{LD}_{50} > 1000 \mu\text{mol/kg}$) in mice²⁷. This list was later expanded by Coenen and colleagues with 2-fluorotyrosine²⁸, which was shown to be rapidly incorporated into proteins²⁸. This data suggests that incorporating fluorinated amino acids into proteins in cultured mammalian cells might be efficient and feasible. Adding fluorinated amino acids to readily available formulations of cell culture media would yield fractionally labeled proteins, where only a fraction of the supplied fluorinated aromatic amino acid would be incorporated into each protein. Yet, the ensemble would have the representation of every position in a given overexpressed (and purified) protein, or all endogenously expressed proteins. Fractional labeling reduces the impact of fluorination on structure and function²⁹ and thereby compensates for the accompanying reduced signal intensity.

Structurally 4-fluorophenylalanine is most similar to phenylalanine, but due the high electronegativity of the fluorine atom, functionally it bears resemblance to tyrosine as well. Thus, it is conceivable that 4-fluorophenylalanine might be incorporated into the position of tyrosine with similar preference to phenylalanine; this depends on which tRNA can accommodate 4-fluorophenylalanine. However, several studies around 1960 suggested that 4-fluorophenylalanine displays a strong preference to replace phenylalanine in animals and in bacteria^{23,30–32}.

To confirm this preference for incorporation of 4-fluorophenylalanine for bacterial expression, we expressed the protein G B1 domain (GB1)³³ in *E. coli* in a media where 4-fluorophenylalanine was added, either as a replacement for phenylalanine or tyrosine, in two individual experiments. The synthesis of aromatic amino acids was inhibited ~30 minutes prior to induction of protein expression by the addition of glyphosate³⁴. We then used two

different labeling schemes to produce 4-fluorophenylalanine labeled GB1. In case 1) 70mg/L tryptophan, 70 mg/L tyrosine and 35 mg/L 4-fluorophenylalanine were supplied with the purpose to replace both phenylalanine sites in GB1 with the fluorinated residue. In case 2) 70 mg/L tryptophan, 70 mg/L phenylalanine and 35 mg/L 4-fluorophenylalanine were supplied to explore whether 4-fluorophenylalanine would be incorporated into the three tyrosine sites in GB1. In Fig. 2a sample-1 corresponds to the blue spectrum and sample-2 corresponds to the red spectrum. In sample-1, 4-fluorophenylalanine is expected to take the positions of the two phenylalanine residues of GB1 (Fig. 2b), but there are three resonances in the 1D ^{19}F NMR spectrum. The downfield resonance at -111.38 ppm is double the height of the two upfield resonances, indicating that the upfield resonances correspond to two conformers of the same 4-fluorophenylalanine, which are in slow exchange on the NMR timescale³⁵. In sample-2, 4-fluorophenylalanine is expected to incorporate into the positions of the three tyrosine residues, instead there are only two weak signals. These resonances are at the same frequencies as two of the resonances observed in the case of sample-1 and the peak intensity is approximately 10% of what was observed for sample-1, indicating about 10% incorporation. Since there are three tyrosines in the GB1 sequence and we observed only two signals, which share their resonance frequencies with two of the resonances observed for the phenylalanine positions, we conclude that 4-fluorophenylalanine was not incorporated into tyrosine positions. Instead, the 4-fluorophenylalanine competed with the phenylalanine added in 2-fold excess. Remarkably, the upfield resonance is not split in sample-2, where the fraction of 4-fluorophenylalanine substituting for phenylalanine is low. This indicates that the two conformations of the phenylalanine responsible for the upfield resonances do not occur naturally. The two conformations are enforced by the presence of the second 4-fluorophenylalanine. As discussed above, at a low percentage of incorporation, only one 4-fluorophenylalanine is expected to be incorporated - the protein is fractionally labeled²⁹ - into one protein and therefore the effect on the structure and function of the protein under study can be minimized.

Fluorine NMR of nucleic acids:

Fluorinated nucleosides, like their amino acid counterparts, were a popular research topic in the 1950s. Nucleocidin, one of only five known naturally occurring organofluorine compounds³⁶, was recognized for its antibiotic activity³⁷ and 5-fluorouracil was shown to exhibit tumor-inhibitory activity³⁸. Since then, many fluorinated nucleoside analogues have been approved by the FDA for their anticancer and antiviral activities^{39,40}. More recently, fluorinated nucleotides have been incorporated into siRNAs and anti-miRNA oligonucleotides³⁶, some with considerable therapeutic potential⁴¹.

The incorporation of ^{19}F substitutions into nucleobases was demonstrated to be non-perturbing by several research groups^{42–44}. Thus, ^{19}F substituted nucleobases provide sensitive NMR reporters to monitor molecular interactions and conformational changes of nucleic acids. ^{19}F NMR is an increasingly popular method to investigate nucleic acids and examples of successful applications include, the measurement of weak interactions⁴⁵, RNA catalysis⁴⁶, nucleic acid folding⁴⁷, DNA methylation⁴⁸, site-specific RNA binding⁴⁹, RNA invasion⁵⁰ and the investigation of telomeric RNA G-quadruplex structures *in vitro* and in

living cells⁵¹. RNAs are substantially more dynamic and have less proton density than proteins. In addition, resonances from imino- and amino-protons are often obscured by exchange processes⁵². Thus, fluorine resonances can act as an additional source of information for structural and functional studies. Despite the tremendous chemical shift distribution of ¹⁹F (~100-fold larger than of ¹H)⁵³, CSA induced line broadening of fluorine resonances limits the application of 1D ¹⁹F NMR for large nucleic acids, similar to what is observed for proteins. Here too, labeling of the aromatic nucleobases with ¹⁹F-¹³C pairs provides an opportunity to disperse the ¹⁹F 1D spectrum into a second ¹³C dimension with narrow TROSY linewidth¹²¹. Theoretical calculations for the 2-fluoroadenine ¹⁹F-¹³C TROSY predict an exceptionally narrow ¹³C linewidth of <1 Hz for nucleic acids tumbling with a correlation time of 25 nanoseconds at 600 MHz¹³. Thus, analogous to proteins, the aromatic ¹⁹F-¹³C TROSY offers new opportunities for the observation of nucleic acid function and structure.

Assignment of fluorine substituted aromatic amino acids and nucleobases:

Fluorinated amino acids and nucleotides have tremendous potential to monitor the interactions and conformational motions of proteins and nucleic acids, but to faithfully deconvolute the information obtained from several fluorine probes it is imperative to assign their resonances unambiguously.

Common strategies to assign ¹⁹F resonances of fluorinated amino acids rely on the use of site-directed mutagenesis of the relevant residue, or residues in the immediate vicinity of the fluorine bearing residue⁷. More sophisticated approaches include the HCCF-COSY experiment⁵⁴, heteronuclear NOESY (HOESY) between ¹⁹F and ¹H resonances⁵⁵, experiments that exploit the scalar coupling between the fluorine nucleus and adjacent aromatic protons⁵⁶ and solvent-induced isotope shift experiments to evaluate solvent accessibility^{57,58}. A new approach, inspired by the aromatic ¹⁹F-¹³C TROSY, could take advantage of the slow relaxation of the ¹⁹F-bonded aromatic ¹³C, by correlating the ¹³C and not ¹⁹F resonances to nearby aromatic carbons through scalar coupling. Using a combination of Total Correlation Spectroscopy (TOCSY) and Correlated Spectroscopy (COSY) transfers, the carbon that is connected to ¹⁹F could be correlated to the backbone carbon. Alternatively, magnetization transfer from fluorine to neighboring protons either using scalar couplings or dipolar couplings could be used to derive assignments. The correlated proton could then be used for further correlation to nearby heteronuclei through scalar couplings. We envision this experiment to be implemented as a 4-dimensional experiment, where an aromatic ¹⁹F-¹³C TROSY would be correlated using heteronuclear dipolar couplings (HOESY) to a ¹H-¹⁵N or ¹H-¹³C spectrum. For large proteins, specific methyl-labeling could be employed to improve resolution. This method would require assignment of at least the methyl resonances of a protein and some prior knowledge of the structure. Gratifyingly, the assignment of ¹H-¹³C-labeled methyls does not require backbone assignment^{59,60}. In certain cases a homology model will be sufficient to identify the correct correlations and distances measured between aromatic fluorines and methyl protons could even be exploited in structure calculations.

Fluorinated nucleic acids are synthesized either with solid-phase synthesis⁴³, or – in case of RNA – with T7 RNA polymerase catalyzed *in vitro* transcription⁶¹ and in some cases *in*

*vivo*⁶². Solid-phase synthesis of fluorine labeled nucleic acids facilitates assignment, because the substitution pattern is freely chosen. However, as the number of nucleotides that require assignment increases, assignment by single nucleotide labeling can become cumbersome. For the assignment of *in vitro* or *in vivo* transcribed fluorinated RNAs, site-directed mutagenesis can be applied. Assignment of fluorine resonances in fluoropyrimidine substituted RNA can further be achieved by measuring long-range $5J(\text{H1}',\text{F})$ couplings to anomeric H1' protons with ^1H - ^{19}F heteronuclear multiple bond correlation (HMBC) spectroscopy^{1,63}. These measurements can be complemented by ^{19}F , ^{19}F -nuclear Overhauser effect spectroscopy (NOESY) and ^{19}F , ^1H -heteronuclear NOESY (HOESY) experiments⁴². The long-range HMBC experiment benefits from the low sensitivity of the ribose H1' chemical shift to fluorine substitution of the nucleobase, allowing the transfer of H1' assignments obtained on non-fluorinated samples. The introduction of ^{19}F - ^{13}C labeled fluoropyrimidines¹²¹ will further simplify the assignment process, as a ^{13}C nucleus in the $\sim 1.5 \text{ Hz } 5J(\text{H1}',\text{F})$ coupling network will most likely provide for a stronger 4-bond coupling $4J(\text{H1}',^{13}\text{C})$. In large nucleic acids, the slow relaxation of the $^{13}\text{C}_\text{F}$ TROSY component would provide a slowly relaxing probe, coupled to the ribose H1', which would be favorable for assignment and structural and functional characterization.

To assign 2-fluoroadenine, Sochor et al. correlated the fluorine signals to the selectively shifted imino proton resonances of their Watson-Crick base paired uridine counterparts with a ^{19}F , ^1H HOESY experiment⁶⁴. For applications to larger nucleic acids, this approach too could benefit from expansion to a third ^{13}C dimension.

Application of the ^{19}F - ^{13}C TROSY to observe the interactions of fluorine-labeled biomolecules:

The exquisite sensitivity of fluorine nuclei to their surroundings, coupled with their sparsity on proteins and nucleic acids carrying fluorine substituted aromatic amino acids or nucleobases, make them particularly well suited for the observation of weak interactions and as probes in drug discovery screens. In particular, the value of proteins labeled with fluorinated aromatic amino acids has been recognized in NMR-based drug discovery programs. Reflecting this, a protein-observed ^{19}F NMR assay, abbreviated PrOF NMR, was invented for fragment-based ligand discovery (FBLD) and structure-activity relationship (SAR) studies⁶⁵. This approach was recently reviewed by Arntson et al.⁶⁶, and Divakaran et al.⁶⁵ and therefore we will restrict our discussion of the method to a brief overview.

In PrOF NMR, one type of aromatic amino acid is ubiquitously substituted for its fluorine-bearing analogue and the fluorine nuclei serve as probes for ligand binding. The chemical shifts of the fluorine resonances are highly sensitive to the electronic environment, a property that is leveraged by PrOF NMR to detect weak ligand binding. In the context of fragment screening PrOF NMR permits the measurement of dissociation constants for compound ranking and the assignment of ^{19}F resonances facilitates the determination of the binding site. However, in certain instances, incorporation of fluorinated amino acids can prevent ligand binding and the sparse occurrence of aromatic amino acids means that

coverage of the receptor may be incomplete⁶⁵. Thus, PrOF NMR based screens are best applied as a complementary strategy to ¹H based screening⁶⁷.

While the lack of aromatic amino acids on certain surfaces of a protein can be an inconvenience, the binding sites of most proteins are enriched for aromatic amino acids⁶⁶. Importantly, this also applies to GPCR micro-switch regions⁶⁸, where highly conserved NPXXY⁶⁹, CWXP and DRY micro-switch motifs govern the switch between active and inactive conformations⁶⁸. A particularly intriguing aspect of PrOF NMR is the opportunity to screen in protein mixtures⁶⁵. This approach was demonstrated for two small proteins, where a limited number of aromatic fluorine resonances was well resolved in 1D ¹⁹F spectra⁷⁰. It could be easily expanded to mixtures of more or larger proteins, by introducing distinct fluorinated aromatic amino acids in different proteins, taking advantage of the large fluorine chemical shift variations between fluorine substituted aromatic amino acid side chains. Chemical shifts for a set of fluorine substituted aromatic amino acids in aqueous solution collected by Dürr et al.⁷¹ are shown in Table 1. The chemical shifts of single fluorine substituents on the phenyl ring appear around -115 ppm and do not show much variation, but the proximity of the fluorine nucleus to the hydroxyl-group in 3-fluorotyrosine induces a ~20 ppm shift. 5-fluorotryptophan and 6-fluorotryptophan resonances appear between -122 ppm and -124 ppm. These differences facilitate the design of screens in complex systems featuring several fluorinated proteins. For further reading, excellent solution and solid state parameters for ¹⁹F NMR are given by Dürr et al.⁷¹, Grage et al.⁷², and Ycas et al.⁷³

Nonetheless, with increasing protein size the number of aromatic amino acids increases and, driven by the large CSA of aromatic fluorines, the signals broaden rapidly due to relaxation. Consequently, while careful design with distinct fluorinated amino acids can enable the differentiation of alternately labeled proteins, resolving fluorine resonances of any given kind quickly becomes challenging.

On the other hand, careful choice of the fluorine substituted amino acid in combination with the ¹⁹F-¹³C TROSY will enable the screening of multiple challenging targets in the same sample. To screen two homologous proteins with identical binding sites, labeling with 3-fluorotyrosine and 2-fluorotyrosine, respectively, would provide a strategy to screen for allosteric inhibitors that selectively induce a conformational change in one of the two homologues. However, it is important to note that labeling with distinct fluorine substituted amino acids can affect protein structure and function differently. For instance, the 2-fluorotyrosine substitution is more conservative than the 3-fluorotyrosine substitution, as introducing a fluorine next to the hydroxyl-group has a substantial polarizing effect on the latter⁷³. Due to the background free nature of fluorine NMR, it is easily conceivable to design such a screen in cell lysates, thereby moving the conditions of the screen closer to physiological conditions.

The strategies discussed above are not unique to proteins and can be easily implemented to screen small molecule inhibitors of nucleic acids as well. ¹⁹F NMR of nucleic acids is excellently suited for the identification of site-specific binders⁴⁹, and a ¹⁹F-¹³C TROSY approach in combination with variations of the fluorine position on a nucleobase, or the use

of different fluorine-labeled nucleobases would provide excellent opportunities for the design of screens and counter screens in the same sample. As the potential of targeting RNAs with small molecules is increasingly recognized⁷⁴, the introduction of the ¹⁹F-¹³C TROSY to ¹⁹F-RNA observed drug discovery will increase the number and size of RNA targets that can be screened simultaneously and provide site-specific information on binding.

Monitoring dynamics and chemical exchange of proteins and nucleic acids:

Structural changes of proteins and nucleic acids on micro-to-millisecond timescales, such as conformational rearrangements that provide access to ligands^{75,76}, conformational sampling of ligand bound conformations and conformational changes induced by allosteric binding, are critical to the function of biomolecules and drug discovery⁷⁷⁻⁷⁹. NMR spectroscopy is unique in that it can study these dynamic processes in a time-resolved manner at atomic resolution. The observables in these experiments are isotropic chemical shifts, which experience chemical exchange modulated by distinct conformational states of biomolecules⁸⁰ or direct ligand binding³⁵. The importance of dynamics in protein function and the role of NMR in studying these processes was recently reviewed by Tokunaga et al.⁸¹, and Alderson et al.⁸².

The sensitivity of fluorine nuclei to small changes in their environment makes them excellent probes for the investigation of chemical exchange, enabling detailed studies of complex biological processes, such as enzyme catalysis⁸³ or protein folding⁸². To monitor exchange processes that occur on the microsecond-to-millisecond timescale, chemical exchange saturation transfer (CEST) and relaxation dispersion (RD) experiments have recently gained popularity^{35,78}. Applied to ¹⁵N and ¹³C nuclei, CEST resolves slower, millisecond (2.5 ms to 50 ms) dynamics^{78,84} and RD is generally used to resolve dynamics in the range of 40 μ s – 5 ms^{77,85}.

RD experiments track the dependence of the effective transverse relaxation rate, $R_{2,eff}$, on the frequency of chemical shift refocusing pulses⁷⁷. If the magnetic environment of the observed nucleus is altered by a chemical event (such as ligand binding) or a conformational kinetic process (e.g. a conformational rearrangement), then its chemical shift will oscillate between these magnetically distinct environments. Consequently, if the exchange process occurs on a timescale that can be refocused with a Carr-Purcell-Meiboom-Gill (CPMG) train of refocusing pulses, then the effective transverse relaxation rate will depend on the frequency of the refocusing pulses and reveal information about the exchange rate, the population of states, and the chemical shift difference between the states^{35,81}. This implies that in order to access faster motions, the frequency of spin-lock pulses must be increased, which can lead to unwanted heating effects. This has historically limited the accessible timescale to 40 μ s for ¹⁵N nuclei⁸⁵. With modern cryogenically cooled instrumentation, the pulsing frequency can be accelerated and is only limited by the length of the spin-lock pulse that is used to refocus chemical exchange, achieving pulsing rates of 6.4 kHz for ¹⁵N, 16 kHz for ¹³C and 40 kHz for ¹H⁸⁶. Pulsing up to this frequency gives access to motions as fast as 3 μ s for ¹H nuclei⁸⁷ and under super-cooled conditions even nanosecond timescale motions have been observed⁸⁸. Fluorine pulse lengths are comparable to those of ¹H and thus RD experiments with close to 40 kHz pulsing frequency should be achievable. The

extreme sensitivity of fluorine to its environment increases chemical shift variance and therefore the observable exchange contribution to RD, when compared to ^1H nuclei. This can be exploited to push the boundaries further in detecting weak binding and lowly populated 'invisible' conformations. One-dimensional ^{19}F NMR RD experiments have already provided exciting insights into protein function, by sampling dynamics on the low μs timescale^{4,83}.

CEST is a complimentary experiment to RD, but provides information about chemical exchange in a slower time-regime. A very weak magnetic field is used to scan the spectrum⁷⁷ (in this case ^{19}F), while the magnetization remains parallel to the main magnetic field. Consequently, CSA induced relaxation effects do not affect CEST experiments. Resonances corresponding to excited/lowly populated states are not visible, but the effect of their saturation is observed on the ground state resonance. The reduction of the observed magnetization of the ground state, when the excited state is saturated, reports on the kinetics and thermodynamics of the exchange process and the chemical shift of the excited state⁷⁸. The sensitivity of the ^{19}F chemical shift is an added advantage for ^{19}F -CEST experiments.

With the introduction of the ^{19}F - ^{13}C TROSY, fluorine NMR RD and CEST experiments have become accessible for large proteins and nucleic acids. Using pulses designed through optimal control theory to reduce the radio frequency power required to excite resonances dispersed over a large chemical shift range, as demonstrated by Coote et al.⁸⁹, we should be able monitor interactions and dynamics of several dozen fluorinated small molecules, aromatic amino acids and nucleobases simultaneously. Thus, fluorine NMR presents an excellent tool for the newly emerging field of systems NMR⁹⁰, where nucleic acids, proteins and small molecule metabolites or ligands are monitored in a single sample. This is illustrated in figure 3, where the hypothetical binding of small molecules decorated with aromatic and aliphatic fluorines is monitored in a single-sample with a ubiquitously ^{19}F - ^{13}C uracil labeled RNA molecule and a ^{19}F - ^{13}C tyrosine labeled protein. The power of monitoring large nucleic acid-protein complexes in the same sample was recently demonstrated with elegant ^1H - ^{13}C methyl TROSY experiments⁹¹.

In the hypothetical experiment shown in figure 3a, small molecule binding occurs on the fast exchange timescale³⁵ and can be monitored in the form of chemical shift perturbations in 1D ^{19}F spectra of the small molecules (Fig. 3b) and 2D ^{19}F - ^{13}C TROSY spectra of the biomolecules in the same sample (Fig. 3c and 3d). In the illustration, the interaction between the RNA and the protein occurs on a millisecond timescale and the bound states of both biomolecules remain invisible. However, the binding event, its kinetics and the interacting interfaces, can be identified from CEST experiments (Fig. 3c). Complex formation induces a microsecond timescale conformational rearrangement on the protein, which is monitored with an RD experiment (Fig. 3d). Since fluorine NMR is background free, these experiments are also thinkable in cellular or nuclear extracts or even in living cells.

In addition to the systems NMR approach, a multiplex mode of this experiment could be designed. Here, taking advantage of the subdivision of fluorine signals of distinct fluorine substituted molecules, independent reactions or interactions could be monitored in the same sample and with the same experiments.

Ligand observed fluorine NMR:

A major challenge in *in vitro* drug discovery relates to the unpredictable behavior of small molecules and their fragments in assay conditions. Small molecules can self-assemble into a variety of nanoentities and colloidal aggregates⁹² and this propensity is determined by the exact assay conditions, such as ionic strength, solubilizing detergents, pH and temperature. In a typical fragment-based drug discovery (FBDD) screen or during hit validation after an *in-silico* or high-throughput screen, hundreds to thousands of fragments or small molecules are evaluated for binding to a receptor interface. Yet, and this is especially true for compounds coming from *in-silico* and high-throughput screens, the actual hit rate depends largely on the behavior of the ligand in the conditions chosen for screening. This can significantly influence the outcome of a screen, by masking some of the best binders or enhancing the affinity of ligands that do not perform as well under physiological conditions. Thus, a ligand that does well under assay conditions optimized for the receptor and the experimental method, might form aggregates under physiological conditions and compounds with excellent properties under physiological conditions are easily missed due to poor solubility under assay conditions. This leads to a large number of false positives and false negatives in drug discovery screens.

The background free nature of fluorine NMR offers a strategy to address this problem. Fluorine NMR screens can be carried out in complex conditions designed to mimic the interior of a cell, the cell culture medium from which the drugs will be supplied to cells in cell-based experiments, or even blood. Elegant, ligand observed screening strategies have been developed for fluorine NMR. In fluorine reporter assays, weakly binding fluorinated ligands act as ‘spy-reporters’^{93,94}, who take advantage of the large CSA of fluorine, which enables the detection of binding even at a very low fraction of bound spy molecules⁹⁴. The sensitivity of the method to weak binders improves at lower spy molecule concentrations, which is crucial for the identification of fragments from fragment screening programs. n-FABS (n Fluorine Atoms for Biochemical Screening) – a powerful method for substrate- or cofactor- based fluorine NMR screening⁹⁴, was developed to address the low sensitivity of NMR experiments. Analogous to site-specific protein-labeling, CF₃ groups (3-FABS) are introduced into the scaffold of known substrates or cofactors to generate a sharp singlet signal of three magnetically equivalent fluorine atoms. Signal intensity can be further improved with the introduction of additional magnetically equivalent CF₃ groups (n-FABS)⁹⁵. Comprehensive reviews on ligand-based fluorine NMR screening were recently published by Dalvit and co-workers^{96,97}.

Beyond the utilization of ¹⁹F NMR for screening and the use of fluorine as a reporter moiety, it is also worthwhile to consider the direct monitoring of fluorinated small molecules. ¹⁹F nuclei are easily and routinely incorporated into analogue series during structure-activity relationship studies, as chemists thrive to take advantage of their unique properties affecting adsorption, biodistribution, metabolism and excretion⁹⁸. As a consequence, over 50% of ‘blockbuster’ drugs harbor ¹⁹F nuclei⁹⁹, including the cholesterol-lowering drug atorvastatin (Lipitor)¹⁰⁰ and the anti-depressant fluoxetine (Prozac)¹⁰¹. This can be exploited for the investigation of these compounds in complex biological systems. To illustrate this, we measured 1D ¹⁹F fluorine NMR spectra of 50 μM

atorvastatin and 50 μ M fluoxetine in Dulbecco's Modified Eagle Medium (DMEM), a frequently used medium to culture mammalian cells, with and without fetal bovine serum (FBS) (Figure 4). Strong signals can be seen for both compounds with signal to noise (S/N) ratios of 63 and 253 for atorvastatin (Fig. 4A and B, blue) and fluoxetine (Fig. 4C and D, red), respectively. The atorvastatin signal is weaker due to the presence of a single fluorine atom as opposed to a CF_3 group on fluoxetine. In addition, couplings to adjacent protons introduce splitting in the atorvastatin spectrum. This could in principle be addressed with ^1H decoupling, which was not applied here.

Addition of FBS results in significant peak broadening in both spectra, leading to S/N ratios of 14 and 34 for atorvastatin and fluoxetine, respectively. This means that both compounds bind to one or more components of FBS. At least one of these interaction partners of both compounds has been previously identified as bovine serum albumin^{102,103}, which is a major component of FBS. Serum albumins are important carrier proteins in the blood, influencing transportation, distribution and metabolism of small molecules and drugs¹⁰³. Since biological systems lack the ^{19}F nuclei (background free), the same experiment that we conducted in cell culture media is easily transferable to plasma or even blood and could be used to evaluate the binding of drug-candidates to biomolecules in these media.

Small molecule interactions with proteins in the blood play a variety of roles, including protection from oxidation, *in vivo* drug distribution, pharmacokinetic and pharmacodynamic properties¹⁰⁴, the regulation of cellular uptake¹⁰⁵ and targeted delivery to organs, solid tumors and inflamed tissues¹⁰⁶. Fluorine NMR of fluorine harboring small molecules can serve as a label and background free method to determine the parameters that regulate these processes or to screen for optimal carrier protein engagement under physiological or near physiological conditions. In a related approach, Krenzel and colleagues took advantage of the excellent resolution of 18- ^{13}C -oleic acid (OA) methyl peaks in 2D ^1H - ^{13}C Heteronuclear Single Quantum Coherence experiments to detect and characterize nine individual binding sites on human serum albumin (HSA)¹⁰⁸. Competition experiments against OA were then employed to identify the binding sites of several drugs, including rosiglitazone and ibuprofen. The identification of the HSA binding site of rosiglitazone helped explain the slow excretion of this drug from systemic circulation.

Fluorine NMR relaxation dispersion experiments could serve to determine kinetic and thermodynamic parameters of distinct binding events. Small molecule shuttling between cells and potential drug carriers and drug interactions with endogenous drug delivery vehicles, such as lipoproteins or albumin and their synthetic analogs could be investigated. These play an increasing role in clinical settings, as they can be exploited to deliver drugs to tumors and other targets by taking advantage of enhanced macromolecule retention in solid tumors and highly organized ligand-receptor recognition systems^{106,107}. In principle, two-dimensional ^{19}F - ^{13}C TROSY or Heteronuclear Multiple Quantum Coherence experiments, in the case of ^{13}C - $^{19}\text{F}_3$ groups, could provide significant resolution enhancement. However, the synthesis of ^{19}F - ^{13}C labelled small molecules will only be feasible for small molecules that are already of elevated interest.

It is even conceivable to go one step further and monitor interactions of fluorinated compounds with proteins and nucleic acids in living cells. High resolution magic angle spinning (HR-MAS)¹⁰⁹ and comprehensive multiphase (CMP) NMR¹¹⁰ could be used to follow the journey of fluorinated drugs through complex multiphase structures such as plants and tissues¹¹¹. Fluorine NMR could be a strong combination with these methods, because it would reduce the complexity of the signal, which might be exploited to reduce spinning speeds - decreasing the damage inflicted on cells and tissues - that are inherent to these technologies.

A particularly intriguing field of research could be the investigation of fluorinated small molecules in living systems with dissolution dynamic nuclear polarization (d-DNP) NMR¹¹². Improvements in sensitivity would enable measurement of fluorinated molecules *in vivo* at low (non-toxic) concentrations¹¹³ and even enable molecular imaging in living organisms¹¹⁴. The expansion of ¹⁹F NMR of small molecules to a second ¹³C dimension, through novel strategies like the aromatic ¹⁹F-¹³C TROSY will in particular benefit from d-DNP. The high DNP enhancement factor of ¹³C¹¹⁵, would ideally complement the slow transverse relaxation of aromatic ¹⁹F-bonded ¹³C resonances and could be exploited for the analysis of the interactions of small molecules in living cells and the observation of fluorinated drug candidates in living organisms.

Instrumentation:

In terms of instrumentation to detect ¹⁹F, there are a number of options depending on the vendor and the vintage of the instrument. They broadly fall into two classifications, the ability to do ¹⁹F NMR with ¹H decoupling and without ¹H decoupling. In newer style instruments equipped with cryogenic probes, the ¹H coil can be tuned to ¹⁹F and the preamplifier can accommodate the ¹⁹F frequency. The best option would be a probe and spectrometer setup that can do ¹⁹F-detection with ¹H decoupling. ¹H decoupling becomes critical while doing ¹⁹F NMR of small molecules since the ¹J(H,F) couplings can be large and smaller long-range J(H,F) couplings also contribute to the transverse relaxation. ¹H decoupling is also important in RD and CEST experiments.

Conclusions:

A major limitation of biological NMR stems from the reliance on isotopic labeling for the analysis of large biomolecules. This has historically restricted the production of proteins used in NMR studies to bacterial expression in *E. coli*. Unfortunately, expression in *E. coli* fails for the expression of many biologically important proteins, due to the lack of an appropriate folding machinery and/or vast differences to mammalian cells with respect to posttranslational modifications. Recently, production of isotope labeled proteins in insect cells has gained considerable popularity¹¹⁶. However, the production of isotope labeled proteins in insect and mammalian cells remains challenging, in particular if deuteration is also required.

The low toxicity and good incorporation of 4- and 2-fluorophenylalanine and 2-fluorotyrosine in proteins of mammals^{27,28} makes these fluorinated amino acids ideal

candidates for incorporation into challenging and biologically important proteins in mammalian cell culture. In particular, because fluorine NMR generally does not rely on deuteration of the labeled protein. An example of the use of fluorinated aromatic amino acids to investigate challenging systems was recently presented by Bai and colleagues¹¹⁷. 5-fluorotryptophan labeling of cytochrome b5 (cytb5) was exploited to detect interactions of the cytb5 transmembrane domain with the full-length rabbit cytochrome P450 2B4 in peptide-based lipid nanodiscs¹¹⁷.

Finally, fluorine NMR spectroscopy is ideally positioned for systems NMR investigations⁹⁰, where multiple proteins, nucleic acids and small molecules are monitored in the same sample simultaneously (Figure 3). The sparsity of the fluorine signal, the variability of the resonance frequency – by choice of fluorinated amino acid, nucleobase and fluorine position on small molecules – and the lack of background signal from actors that can be kept invisible, should facilitate the design of complex networks while minimizing the number of experiments required to follow the components of the network.

Mechanistic studies of fluorinated nucleic acids, proteins and small molecules in living cells are currently limited by spectrometer sensitivity. However, just like the development of direct electron-detection cameras boosted the resolution of cryo-electron microscopy¹¹⁸ and turned this technology almost overnight into a major force in structural biology, engineering ingenuity could, in the future, propel NMR spectroscopy and MRI to the forefront of mechanistic elucidation in living cells, tissues and organisms.

Materials and Methods:

Expression and purification of fluorine-labeled proteins:

BL21 (DE3) *E. coli* were transformed with plasmids encoding the protein G B1 domain (GB1; pET9d). Cultures were grown at 37 °C in a shaker-incubator in M9 minimal medium supplemented with 1 g/L ¹⁵NH₄Cl. To achieve uniform incorporation of 4-¹⁹F phenylalanine, cells were first grown to an optical density of 0.5 measured at a wavelength of 600 nm (OD₆₀₀). Then 1 g/L glyphosate was added, along with 35 mg/L 4-¹⁹F L-phenylalanine (Alfa Aesar, 4-fluoro-L-phenylalanine, L19934), 70 mg/L L-tryptophan and 70 mg/L L-phenylalanine or L-tyrosine. Cultures were then grown to an OD₆₀₀ of 0.7–0.8 at which point protein expression was induced with 1 mM isopropyl β-D-1-thiogalactopyranoside (IPTG). The cultures were incubated for an additional 16 h at 25 °C to allow for protein expression. Cells were pelleted by centrifugation for 20 min at 4 °C at 3,500 x *g*.

Cell pellets were resuspended in 40 mL of GB1 lysis buffer (50 mM Tris-HCl (pH 8.0), 350 mM NaCl, 10 mM imidazole, 5 mM β-mercaptoethanol (β-ME)) per liter of original bacterial culture and lysed by sonication. Cell debris was removed from the crude lysate by centrifugation at 4 °C for 40 min at 33,000 x *g*. GB1 was purified from the resulting supernatant by gravity-flow affinity chromatography using 5 mL (10-mL of a 50% slurry) of Ni-NTA resin (Qiagen). After washing the resin with 40 mL of 50 mM Tris-HCl (pH 8.0), 350 mM NaCl and 40 mM imidazole, the protein was eluted in an identical buffer containing 350 mM imidazole. GB1 was then further purified using size exclusion chromatography on a

Superdex 75 10/300 GL (GE Healthcare Life Sciences) column equilibrated in phosphate buffered saline, buffer exchanged into NMR buffer (10 mM Na₂HPO₄ (pH 6.5), 50 mM NaCl, 1mM EDTA) with an Amicon® Ultra-15 centrifugal filter unit with 3000 Dalton nominal molecular weight limit (Millipore Sigma) and concentrated to 1.5 mM for NMR spectroscopy.

The ¹⁹F-¹³C 3-Fluorotyrosine labeled α7 single-ring of the 20S proteasome core particle (CP) from *Thermoplasma acidophilum* was prepared as described previously¹³.

NMR spectroscopy:

1D ¹⁹F NMR spectra of 4-¹⁹F phenylalanine labeled GB1 samples were recorded on a 600 MHz Bruker spectrometer equipped with an AVANCE 4 console and a cryogenically cooled QCIF probe.

50 μM atorvastatin (TCI America, atorvastatin calcium salt trihydrate, A2476) and 50 μM fluoxetine (TCI America, fluoxetine hydrochloride, F0750) were prepared in DMEM (Gibco, cat. #11995–065) supplemented with 70 mM HEPES, 90 mM glucose and 20% D₂O, as described by Barbieri et al.¹¹⁹, in presence or absence of 10% FBS (Gibco, cat. #10438–026).

1D ¹⁹F NMR spectra of the compounds were recorded on a 600 MHz Bruker spectrometer equipped with an AVANCE II console and a Prodigy TCI cryoprobe that is tuneable to ¹⁹F. The ¹H channel was tuned to ¹⁹F and therefore ¹H decoupling was not possible.

2D ¹⁹F-¹³C TROSYs of 1 mM proteasome single-ring α7 particle were recorded as ¹³C-detected, ¹⁹F-¹³C out-and-stay TROSYs. 2 mM CQ (Millipore Sigma, Chloroquine diphosphate salt, C6628) was added from a 100 mM stock in double-distilled water. Spectra were recorded on a 600 MHz (¹H frequency) Bruker spectrometer equipped with a 5mm inverse triple resonance CryoProbe (TCI, H tuneable to F) with ¹H/¹⁹F, ¹³C and ¹⁵N frequencies. The ¹H channel was tuned to ¹⁹F.

Acknowledgments:

The authors would like to thank Gregory Heffron (Associate in Biological Chemistry and Molecular Pharmacology, Harvard Medical School, Boston, MA, USA) and the East Quad NMR Facility at Harvard Medical School, as well as Clemens Anklin (Bruker Biospin, Billerica, MA, USA), for assistance with fluorine NMR. The authors are especially grateful to Vladimir M. Gelev (Faculty of Chemistry and Pharmacy, Sofia University, Sofia, Bulgaria) for the synthesis of ¹⁹F-¹³C-labeled 3-fluorotyrosine, to Sandeep Chhabra (Amgen, CA, USA) for the expression and purification of the proteasome α7 single-ring subunit, to L.E. Kay (Departments of Molecular Genetics, Biochemistry, and Chemistry, University of Toronto, Toronto, Ontario, Canada) for sharing the plasmid carrying the single-ring α7 proteasome particle with us and to Helena Kovacs (Bruker Biospin, Fällanden, Switzerland) for discussions regarding the work.

Funding: This research was supported by the NIH grant GM129026 to G.W. A.B. acknowledges funding from the American Heart Association's fellowship 19POST34380800 and the Austrian Science Fund's Schrödinger Fellowship J3872-B21. H.A. thanks the Claudia Adams Barr Program for Innovative Cancer Research for support.

References:

1. Hennig M, Munzarova ML, Bermel W, Scott LG, Sklenar V & Williamson JR Measurement of long-range ^1H - ^{19}F scalar coupling constants and their glycosidic torsion dependence in 5-fluoropyrimidine-substituted RNA. *J Am Chem Soc* 128, 5851–8 (2006). [PubMed: 16637654]
2. Ye L, Van Eps N, Zimmer M, Ernst OP & Prosser RS Activation of the A2A adenosine G-protein-coupled receptor by conformational selection. *Nature* 533, 265–8 (2016). [PubMed: 27144352]
3. Liu JJ, Horst R, Katritch V, Stevens RC & Wüthrich K Biased signaling pathways in beta2-adrenergic receptor characterized by ^{19}F -NMR. *Science* 335, 1106–10 (2012). [PubMed: 22267580]
4. Manglik A, Kim TH, Masureel M, Altenbach C, Yang Z, Hilger D, Lerch MT, Kobilka TS, Thian FS, Hubbell WL, Prosser RS & Kobilka BK Structural Insights into the Dynamic Process of beta2-Adrenergic Receptor Signaling. *Cell* 161, 1101–1111 (2015). [PubMed: 25981665]
5. Horst R, Liu JJ, Stevens RC & Wüthrich K β 2-Adrenergic Receptor Activation by Agonists Studied with ^{19}F NMR Spectroscopy. *Angewandte Chemie International Edition* 52, 10762–10765 (2013). [PubMed: 23956158]
6. Kim TH, Chung KY, Manglik A, Hansen AL, Dror RO, Mildorf TJ, Shaw DE, Kobilka BK & Prosser RS The Role of Ligands on the Equilibria Between Functional States of a G Protein-Coupled Receptor. *J Am Chem Soc* 135, 9465–9474 (2013). [PubMed: 23721409]
7. Danielson MA & Falke JJ Use of ^{19}F NMR to probe protein structure and conformational changes. *Annu Rev Biophys Biomol Struct* 25, 163–95 (1996). [PubMed: 8800468]
8. Liu L, Byeon JJ, Bahar I & Gronenborn AM Domain swapping proceeds via complete unfolding: a ^{19}F - and ^1H -NMR study of the Cyanovirin-N protein. *J Am Chem Soc* 134, 4229–35 (2012). [PubMed: 22296296]
9. Schuler B, Kremer W, Kalbitzer HR & Jaenicke R Role of entropy in protein thermostability: folding kinetics of a hyperthermophilic cold shock protein at high temperatures using ^{19}F NMR. *Biochemistry* 41, 11670–80 (2002). [PubMed: 12269809]
10. Toptygin D, Gronenborn AM & Brand L Nanosecond relaxation dynamics of protein GB1 identified by the time-dependent red shift in the fluorescence of tryptophan and 5-fluorotryptophan. *J Phys Chem B* 110, 26292–302 (2006). [PubMed: 17181288]
11. Yang F, Yu X, Liu C, Qu C-X, Gong Z, Liu H-D, Li F-H, Wang H-M, He D-F, Yi F, Song C, Tian C-L, Xiao K-H, Wang J-Y & Sun J-P Phospho-selective mechanisms of arrestin conformations and functions revealed by unnatural amino acid incorporation and ^{19}F -NMR. *Nature Communications* 6, 8202 (2015).
12. Dalvit C, Papeo G, Mongelli N, Giordano P, Saccardo B, Costa A, Veronesi M & Ko SY Rapid NMR-based functional screening and IC50 measurements performed at unprecedentedly low enzyme concentration. *Drug Development Research* 64, 105–113 (2005).
13. Boeszoermenyi A, Chhabra S, Dubey A, Radeva DL, Burdzhiev NT, Chanev CD, Petrov OI, Gelev VM, Zhang M, Anklin C, Kovacs H, Wagner G, Kuprov I, Takeuchi K & Arthanari H Aromatic (^{19}F) - (^{13}C) TROSY: a background-free approach to probe biomolecular structure, function, and dynamics. *Nat Methods* 16, 333–340 (2019). [PubMed: 30858598]
14. Milbradt AG, Arthanari H, Takeuchi K, Boeszoermenyi A, Hagn F & Wagner G Increased resolution of aromatic cross peaks using alternate ^{13}C labeling and TROSY. *J Biomol NMR* 62, 291–301 (2015). [PubMed: 25957757]
15. Pervushin K, Riek R, Wider G & Wüthrich K Transverse Relaxation-Optimized Spectroscopy (TROSY) for NMR Studies of Aromatic Spin Systems in ^{13}C -Labeled Proteins. *Journal of the American Chemical Society* 120, 6394–6400 (1998).
16. Sprangers R, Li X, Mao X, Rubinstein JL, Schimmer AD & Kay LE TROSY-based NMR evidence for a novel class of 20S proteasome inhibitors. *Biochemistry* 47, 6727–34 (2008). [PubMed: 18540636]
17. Chrominski M, Baranowski MR, Chmielinski S, Kowalska J & Jemielity J Synthesis of Trifluoromethylated Purine Ribonucleotides and Their Evaluation as (^{19}F) NMR Probes. *J Org Chem* 85, 3440–3453 (2020). [PubMed: 31994393]

18. Wang M, Lu M, Fritz MP, Quinn CM, Byeon IL, Byeon CH, Struppe J, Maas W, Gronenborn AM & Polenova T Fast Magic-Angle Spinning (19)F NMR Spectroscopy of HIV-1 Capsid Protein Assemblies. *Angew Chem Int Ed Engl* 57, 16375–16379 (2018). [PubMed: 30225969]
19. Roos M, Mandala VS & Hong M Determination of Long-Range Distances by Fast Magic-Angle-Spinning Radiofrequency-Driven (19)F-(19)F Dipolar Recoupling NMR. *J Phys Chem B* 122, 9302–9313 (2018). [PubMed: 30211552]
20. Cohen GN & Gros F PROTEIN BIOSYNTHESIS. *Annual Review of Biochemistry* 29, 525–546 (1960).
21. Kruh J & Rosa J Incorporation in vitro de [14C]fluorophénylalanine dans l'hémoglobine des réticulocytes de lapin. *Biochimica et Biophysica Acta* 34, 561–563 (1959). [PubMed: 14412245]
22. Vaughan M & Steinberg D Biosynthetic incorporation of fluorophenylalanine into crystalline proteins. *Biochimica et biophysica acta* 40, 230–236 (1960). [PubMed: 13841479]
23. Westhead EW & Boyer PD The incorporation of p-fluorophenylalanine into some rabbit enzymes and other proteins. *Biochimica et Biophysica Acta* 54, 145–156 (1961). [PubMed: 14006343]
24. Garzo T, Hansson E & Ullberg S Uptake of C-14-para-fluorophenylalanine in the tissues of mice. *Experientia* 18, 43–4 (1962). [PubMed: 13897129]
25. Hansson E & Garzo T Amino acid-analogue incorporation into pancreatic juice proteins in vivo. *Biochim Biophys Acta* 61, 121–8 (1962). [PubMed: 13904473]
26. Bodsch W, Coenen HH, Stocklin G, Takahashi K & Hossmann KA Biochemical and autoradiographic study of cerebral protein synthesis with [18F]-and [14C]fluorophenylalanine. *J Neurochem* 50, 979–83 (1988). [PubMed: 3339368]
27. Weissman A & Koe BK m-Fluorotyrosine convulsions and mortality: relationship to catecholamine and citrate metabolism. *J Pharmacol Exp Ther* 155, 135–44 (1967). [PubMed: 5297377]
28. Coenen HH, Kling P & Stocklin G Cerebral metabolism of L-[2-18F]fluorotyrosine, a new PET tracer of protein synthesis. *J Nucl Med* 30, 1367–72 (1989). [PubMed: 2787848]
29. Kiteviski-LeBlanc JL, Evancics F & Scott Prosser R Optimizing (1)(9)F NMR protein spectroscopy by fractional biosynthetic labeling. *J Biomol NMR* 48, 113–21 (2010). [PubMed: 20734112]
30. Munier R & Cohen GN Incorporation d'analogues structuraux d'aminoacides dans les protéines bactériennes au cours de leur synthèse in vivo. *Biochimica et Biophysica Acta* 31, 378–391 (1959). [PubMed: 13628664]
31. Richmond MH Incorporation of dl-beta-(p-fluorophenyl)[beta-C]alanine into exopenicillinase by *Bacillus cereus* 569/H. *Biochem J* 77, 121–35 (1960). [PubMed: 16748837]
32. Yoshida A Studies on the mechanism of protein synthesis; Incorporation of p-fluorophenylalanine into α -amylase of *Bacillus subtilis*. *Biochimica et Biophysica Acta* 41, 98–103 (1960). [PubMed: 13846573]
33. Gronenborn AM, Filpula DR, Essig NZ, Achari A, Whitlow M, Wingfield PT & Clore GM A novel, highly stable fold of the immunoglobulin binding domain of streptococcal protein G. *Science* 253, 657–61 (1991). [PubMed: 1871600]
34. Kim H-W, Perez JA, Ferguson SJ & Campbell ID The specific incorporation of labelled aromatic amino acids into proteins through growth of bacteria in the presence of glyphosate. *FEBS Letters* 272, 34–36 (1990). [PubMed: 2146161]
35. Palmer AG 3rd, Kroenke CD & Loria JP Nuclear magnetic resonance methods for quantifying microsecond-to-millisecond motions in biological macromolecules. *Methods Enzymol* 339, 204–38 (2001). [PubMed: 11462813]
36. Guo F, Li Q & Zhou C Synthesis and biological applications of fluoro-modified nucleic acids. *Org Biomol Chem* 15, 9552–9565 (2017). [PubMed: 29086791]
37. Hewitt RI, Gumble AR, Taylor LH & Wallace WS The activity of a new antibiotic, nucleocidin, in experimental infections with *Trypanosoma equiperdum*. *Antibiot Annu*, 722–9 (1956). [PubMed: 13425455]
38. Heidelberg C, Chaudhuri NK, Danneberg P, Mooren D, Griesbach L, Duschinsky R, Schnitzer RJ, Plevin E & Scheiner J Fluorinated pyrimidines, a new class of tumour-inhibitory compounds. *Nature* 179, 663–6 (1957). [PubMed: 13418758]
39. Liu P, Sharon A & Chu CK Fluorinated Nucleosides: Synthesis and Biological Implication. *J Fluor Chem* 129, 743–766 (2008). [PubMed: 19727318]

40. Qiu X-L, Xu X-H & Qing F-L Recent advances in the synthesis of fluorinated nucleosides. *Tetrahedron* 66, 789–843 (2010).
41. Rayner KJ, Esau CC, Hussain FN, McDaniel AL, Marshall SM, van Gils JM, Ray TD, Sheedy FJ, Goedeke L, Liu X, Khatsenko OG, Kaimal V, Lees CJ, Fernandez-Hernando C, Fisher EA, Temel RE & Moore KJ Inhibition of miR-33a/b in non-human primates raises plasma HDL and lowers VLDL triglycerides. *Nature* 478, 404–7 (2011). [PubMed: 22012398]
42. Hennig M, Scott LG, Sperling E, Bermel W & Williamson JR Synthesis of 5-fluoropyrimidine nucleotides as sensitive NMR probes of RNA structure. *J Am Chem Soc* 129, 14911–21 (2007). [PubMed: 17990877]
43. Puffer B, Kreutz C, Rieder U, Ebert MO, Konrat R & Micura R 5-Fluoro pyrimidines: labels to probe DNA and RNA secondary structures by 1D 19F NMR spectroscopy. *Nucleic Acids Res* 37, 7728–40 (2009). [PubMed: 19843610]
44. Scott LG, Geierstanger BH, Williamson JR & Hennig M Enzymatic synthesis and 19F NMR studies of 2-fluoroadenine-substituted RNA. *J Am Chem Soc* 126, 11776–7 (2004). [PubMed: 15382896]
45. Olejniczak M, Gdaniec Z, Fischer A, Grabarkiewicz T, Bielecki L & Adamiak RW The bulge region of HIV-1 TAR RNA binds metal ions in solution. *Nucleic Acids Res* 30, 4241–9 (2002). [PubMed: 12364603]
46. Carlomagno T, Amata I, Codutti L, Falb M, Fohrer J, Masiewicz P & Simon B Structural principles of RNA catalysis in a 2'–5' lariat-forming ribozyme. *J Am Chem Soc* 135, 4403–11 (2013). [PubMed: 23472843]
47. Hammann C, Norman DG & Lilley DM Dissection of the ion-induced folding of the hammerhead ribozyme using 19F NMR. *Proc Natl Acad Sci U S A* 98, 5503–8 (2001). [PubMed: 11331743]
48. Klimasauskas S, Szyperski T, Serva S & Wuthrich K Dynamic modes of the flipped-out cytosine during HhaI methyltransferase-DNA interactions in solution. *EMBO J* 17, 317–24 (1998). [PubMed: 9427765]
49. Kreutz C, Kahlig H, Konrat R & Micura R A general approach for the identification of site-specific RNA binders by 19F NMR spectroscopy: proof of concept. *Angew Chem Int Ed Engl* 45, 3450–3 (2006). [PubMed: 16622887]
50. Kiviniemi A & Virta P Characterization of RNA invasion by (19)F NMR spectroscopy. *J Am Chem Soc* 132, 8560–2 (2010). [PubMed: 20521791]
51. Bao HL, Ishizuka T, Sakamoto T, Fujimoto K, Uechi T, Kenmochi N & Xu Y Characterization of human telomere RNA G-quadruplex structures in vitro and in living cells using 19F NMR spectroscopy. *Nucleic Acids Res* 45, 5501–5511 (2017). [PubMed: 28180296]
52. Schnieders R, Keyhani S, Schwalbe H & Fürtig B More than Proton Detection—New Avenues for NMR Spectroscopy of RNA. *Chemistry – A European Journal* 26, 102–113 (2020).
53. Kitevski-LeBlanc JL & Prosser RS Current applications of 19F NMR to studies of protein structure and dynamics. *Progress in Nuclear Magnetic Resonance Spectroscopy* 62, 1–33 (2012). [PubMed: 22364614]
54. Kitevski-LeBlanc JL, Al-Abdul-Wahid MS & Prosser RS A mutagenesis-free approach to assignment of (19)F NMR resonances in biosynthetically labeled proteins. *J Am Chem Soc* 131, 2054–5 (2009). [PubMed: 19173647]
55. Watts JK, Martin-Pintado N, Gomez-Pinto I, Schwartzentruber J, Portella G, Orozco M, Gonzalez C & Damha MJ Differential stability of 2'F-ANA*RNA and ANA*RNA hybrid duplexes: roles of structure, pseudohydrogen bonding, hydration, ion uptake and flexibility. *Nucleic Acids Res* 38, 2498–511 (2010). [PubMed: 20071751]
56. Kitevski-LeBlanc JL, Evancis F & Scott Prosser R Approaches to the assignment of 19F resonances from 3-fluorophenylalanine labeled calmodulin using solution state NMR. *J Biomol NMR* 47, 113–123 (2010). [PubMed: 20401735]
57. Khan F, Kuprov I, Craggs TD, Hore PJ & Jackson SE 19F NMR studies of the native and denatured states of green fluorescent protein. *J Am Chem Soc* 128, 10729–37 (2006). [PubMed: 16910667]
58. Kitevski-LeBlanc JL, Evancis F & Prosser RS Approaches for the measurement of solvent exposure in proteins by 19F NMR. *J Biomol NMR* 45, 255–64 (2009). [PubMed: 19655092]

59. Pritisanac I, Degiacomi MT, Alderson TR, Carneiro MG, Ab E, Siegal G & Baldwin AJ Automatic Assignment of Methyl-NMR Spectra of Supramolecular Machines Using Graph Theory. *J Am Chem Soc* 139, 9523–9533 (2017). [PubMed: 28691806]
60. Pritisanac I, Wurz JM, Alderson TR & Guntert P Automatic structure-based NMR methyl resonance assignment in large proteins. *Nat Commun* 10, 4922 (2019). [PubMed: 31664028]
61. Guillerez J, Lopez PJ, Proux F, Launay H & Dreyfus M A mutation in T7 RNA polymerase that facilitates promoter clearance. *Proc Natl Acad Sci U S A* 102, 5958–63 (2005). [PubMed: 15831591]
62. Horowitz J, Ou CN & Ishaq M Isolation and partial characterization of Escherichia coli valine transfer RNA with uridine-derived residues replaced by 5-fluorouridine. *J Mol Biol* 88, 301–12 (1974). [PubMed: 4616086]
63. Scott LG & Hennig M Chapter Three - 19F-Site-Specific-Labeled Nucleotides for Nucleic Acid Structural Analysis by NMR in *Methods in Enzymology*, Vol. 566 (ed. Kelman Z) 59–87 (Academic Press, 2016). [PubMed: 26791976]
64. Sochor F, Silvers R, Muller D, Richter C, Furtig B & Schwalbe H (19)F-labeling of the adenine H2-site to study large RNAs by NMR spectroscopy. *J Biomol NMR* 64, 63–74 (2016). [PubMed: 26704707]
65. Divakaran A, Kirberger SE & Pomerantz WCK SAR by (Protein-Observed) (19)F NMR. *Acc Chem Res* 52, 3407–3418 (2019). [PubMed: 31718149]
66. Arntson KE & Pomerantz WC Protein-Observed Fluorine NMR: A Bioorthogonal Approach for Small Molecule Discovery. *J Med Chem* 59, 5158–71 (2016). [PubMed: 26599421]
67. Johnson JA, Nicolaou CA, Kirberger SE, Pandey AK, Hu H & Pomerantz WCK Evaluating the Advantages of Using 3D-Enriched Fragments for Targeting BET Bromodomains. *ACS Med Chem Lett* 10, 1648–1654 (2019). [PubMed: 31857841]
68. Nygaard R, Frimurer TM, Holst B, Rosenkilde MM & Schwartz TW Ligand binding and micro-switches in 7TM receptor structures. *Trends Pharmacol Sci* 30, 249–59 (2009). [PubMed: 19375807]
69. Venkatakrishnan AJ, Deupi X, Lebon G, Heydenreich FM, Flock T, Miljus T, Balaji S, Bouvier M, Veprintsev DB, Tate CG, Schertler GF & Babu MM Diverse activation pathways in class A GPCRs converge near the G-protein-coupling region. *Nature* 536, 484–7 (2016). [PubMed: 27525504]
70. Urick AK, Hawk LM, Cassel MK, Mishra NK, Liu S, Adhikari N, Zhang W, dos Santos CO, Hall JL & Pomerantz WC Dual Screening of BPTF and Brd4 Using Protein-Observed Fluorine NMR Uncovers New Bromodomain Probe Molecules. *ACS Chem Biol* 10, 2246–56 (2015). [PubMed: 26158404]
71. Durr UH, Grage SL, Witter R & Ulrich AS Solid state 19F NMR parameters of fluorine-labeled amino acids. Part I: aromatic substituents. *J Magn Reson* 191, 7–15 (2008). [PubMed: 18155936]
72. Grage SL, Durr UH, Afonin S, Mikhailiuk PK, Komarov IV & Ulrich AS Solid state 19F NMR parameters of fluorine-labeled amino acids. Part II: aliphatic substituents. *J Magn Reson* 191, 16–23 (2008). [PubMed: 18155628]
73. Ycas PD, Wagner N, Olsen NM, Fu R & Pomerantz WCK 2-Fluorotyrosine is a valuable but understudied amino acid for protein-observed (19)F NMR. *J Biomol NMR* 74, 61–69 (2020). [PubMed: 31760571]
74. Rizvi NF, Santa Maria JP Jr., Nahvi A, Klappenbach J, Klein DJ, Curran PJ, Richards MP, Chamberlin C, Saradjian P, Burchard J, Aguilar R, Lee JT, Dandliker PJ, Smith GF, Kutchukian P & Nickbarg EB Targeting RNA with Small Molecules: Identification of Selective, RNA-Binding Small Molecules Occupying Drug-Like Chemical Space. *SLAS Discov* 25, 384–396 (2020). [PubMed: 31701793]
75. Miskei M, Gregus A, Sharma R, Duro N, Zsolyomi F & Fuxreiter M Fuzziness enables context dependence of protein interactions. *FEBS Lett* 591, 2682–2695 (2017). [PubMed: 28762260]
76. Mulder FA, Skrynnikov NR, Hon B, Dahlquist FW & Kay LE Measurement of slow (micro-s-ms) time scale dynamics in protein side chains by (15)N relaxation dispersion NMR spectroscopy: application to Asn and Gln residues in a cavity mutant of T4 lysozyme. *J Am Chem Soc* 123, 967–75 (2001). [PubMed: 11456632]

77. Kay LE New Views of Functionally Dynamic Proteins by Solution NMR Spectroscopy. *J Mol Biol* 428, 323–331 (2016). [PubMed: 26707200]
78. Vallurupalli P, Bouvignies G & Kay LE Studying “invisible” excited protein states in slow exchange with a major state conformation. *J Am Chem Soc* 134, 8148–61 (2012). [PubMed: 22554188]
79. Waudby CA, Ramos A, Cabrita LD & Christodoulou J Two-Dimensional NMR Lineshape Analysis. *Sci Rep* 6, 24826 (2016). [PubMed: 27109776]
80. Ban D, Smith CA, de Groot BL, Griesinger C & Lee D Recent advances in measuring the kinetics of biomolecules by NMR relaxation dispersion spectroscopy. *Arch Biochem Biophys* 628, 81–91 (2017). [PubMed: 28576576]
81. Tokunaga Y, Viennet T, Arthanari H & Takeuchi K Spotlight on the Ballet of Proteins: The Structural Dynamic Properties of Proteins Illuminated by Solution NMR. *Int J Mol Sci* 21(2020).
82. Alderson TR & Kay LE Unveiling invisible protein states with NMR spectroscopy. *Current Opinion in Structural Biology* 60, 39–49 (2020). [PubMed: 31835059]
83. Kim TH, Mehrabi P, Ren Z, Sljoka A, Ing C, Bezginov A, Ye L, Pomes R, Prosser RS & Pai EF The role of dimer asymmetry and protomer dynamics in enzyme catalysis. *Science* 355(2017).
84. Bouvignies G & Kay LEA 2D (1)3C-CEST experiment for studying slowly exchanging protein systems using methyl probes: an application to protein folding. *J Biomol NMR* 53, 303–10 (2012). [PubMed: 22689067]
85. Ban D, Gossert AD, Giller K, Becker S, Griesinger C & Lee D Exceeding the limit of dynamics studies on biomolecules using high spin-lock field strengths with a cryogenically cooled probehead. *J Magn Reson* 221, 1–4 (2012). [PubMed: 22743535]
86. Reddy JG, Pratihari S, Ban D, Frischkorn S, Becker S, Griesinger C & Lee D Simultaneous determination of fast and slow dynamics in molecules using extreme CPMG relaxation dispersion experiments. *J Biomol NMR* 70, 1–9 (2018). [PubMed: 29188417]
87. Smith CA, Ban D, Pratihari S, Giller K, Schwiegk C, de Groot BL, Becker S, Griesinger C & Lee D Population shuffling of protein conformations. *Angew Chem Int Ed Engl* 54, 207–10 (2015). [PubMed: 25377083]
88. Pratihari S, Sabo TM, Ban D, Fenwick RB, Becker S, Salvatella X, Griesinger C & Lee D Kinetics of the Antibody Recognition Site in the Third IgG-Binding Domain of Protein G. *Angew Chem Int Ed Engl* 55, 9567–70 (2016). [PubMed: 27345359]
89. Coote P, Anklin C, Masefski W, Wagner G & Arthanari H Rapid convergence of optimal control in NMR using numerically-constructed toggling frames. *J Magn Reson* 281, 94–103 (2017). [PubMed: 28578162]
90. Nikolaev Y, Ripin N, Soste M, Picotti P, Iber D & Allain FH Systems NMR: single-sample quantification of RNA, proteins and metabolites for biomolecular network analysis. *Nat Methods* 16, 743–749 (2019). [PubMed: 31363225]
91. Abramov G, Velyvis A, Rennella E, Wong LE & Kay LE A methyl-TROSY approach for NMR studies of high-molecular-weight DNA with application to the nucleosome core particle. *Proc Natl Acad Sci U S A* (2020).
92. Ayotte Y, Marando VM, Vaillancourt L, Bouchard P, Heffron G, Coote PW, Larda ST & LaPlante SR Exposing Small-Molecule Nanoentities by a Nuclear Magnetic Resonance Relaxation Assay. *J Med Chem* 62, 7885–7896 (2019). [PubMed: 31422659]
93. Dalvit C, Ardini E, Flocco M, Fogliatto GP, Mongelli N & Veronesi M A general NMR method for rapid, efficient, and reliable biochemical screening. *J Am Chem Soc* 125, 14620–5 (2003). [PubMed: 14624613]
94. Dalvit C, Mongelli N, Papeo G, Giordano P, Veronesi M, Moskau D & Kummerle R Sensitivity improvement in 19F NMR-based screening experiments: theoretical considerations and experimental applications. *J Am Chem Soc* 127, 13380–5 (2005). [PubMed: 16173772]
95. Papeo G, Giordano P, Brasca MG, Buzzo F, Caronni D, Ciprandi F, Mongelli N, Veronesi M, Vulpetti A & Dalvit C Polyfluorinated amino acids for sensitive 19F NMR-based screening and kinetic measurements. *J Am Chem Soc* 129, 5665–72 (2007). [PubMed: 17417847]
96. Dalvit C & Vulpetti A Ligand-Based Fluorine NMR Screening: Principles and Applications in Drug Discovery Projects. *J Med Chem* 62, 2218–2244 (2019). [PubMed: 30295487]

97. Dalvit C, Veronesi M & Vulpetti A Fluorine NMR functional screening: from purified enzymes to human intact living cells. *J Biomol NMR* (2020).
98. Muller K, Faeh C & Diederich F Fluorine in pharmaceuticals: Looking beyond intuition. *Science* 317, 1881–1886 (2007). [PubMed: 17901324]
99. Mei H, Han J, Fustero S, Medio-Simon M, Sedgwick DM, Santi C, Ruzziconi R & Soloshonok VA Fluorine-Containing Drugs Approved by the FDA in 2018. *Chemistry* 25, 11797–11819 (2019). [PubMed: 31099931]
100. Roth BD The discovery and development of atorvastatin, a potent novel hypolipidemic agent. *Prog Med Chem* 40, 1–22 (2002). [PubMed: 12516521]
101. Wong DT, Bymaster FP & Engleman EA Prozac (fluoxetine, lilly 110140), the first selective serotonin uptake inhibitor and an antidepressant drug: Twenty years since its first publication. *Life Sciences* 57, 411–441 (1995). [PubMed: 7623609]
102. Katrahalli U, Jaldappagari S & Kalanur SS Study of the interaction between fluoxetine hydrochloride and bovine serum albumin in the imitated physiological conditions by multi-spectroscopic methods. *Journal of Luminescence* 130, 211–216 (2010).
103. Wang Q, Huang CR, Jiang M, Zhu YY, Wang J, Chen J & Shi JH Binding interaction of atorvastatin with bovine serum albumin: Spectroscopic methods and molecular docking. *Spectrochim Acta A Mol Biomol Spectrosc* 156, 155–63 (2016). [PubMed: 26688207]
104. Yang F, Zhang Y & Liang H Interactive association of drugs binding to human serum albumin. *Int J Mol Sci* 15, 3580–95 (2014). [PubMed: 24583848]
105. Marek M, Silvestro D, Fredslund MD, Andersen TG & Pomorski TG Serum albumin promotes ATP-binding cassette transporter-dependent sterol uptake in yeast. *FEMS Yeast Res* 14, 1223–33 (2014). [PubMed: 25331273]
106. Kratz F Albumin as a drug carrier: design of prodrugs, drug conjugates and nanoparticles. *J Control Release* 132, 171–83 (2008). [PubMed: 18582981]
107. Chaudhary J, Bower J & Corbin IR Lipoprotein Drug Delivery Vehicles for Cancer: Rationale and Reason. *Int J Mol Sci* 20(2019).
108. Krenzel ES, Chen Z & Hamilton JA Correspondence of fatty acid and drug binding sites on human serum albumin: a two-dimensional nuclear magnetic resonance study. *Biochemistry* 52, 1559–67 (2013). [PubMed: 23360066]
109. Maas WE, Laukien FH & Cory DG Gradient, High Resolution, Magic Angle Sample Spinning NMR. *Journal of the American Chemical Society* 118, 13085–13086 (1996).
110. Courtier-Murias D, Farooq H, Masoom H, Botana A, Soong R, Longstaffe JG, Simpson MJ, Maas WE, Fey M, Andrew B, Struppe J, Hutchins H, Krishnamurthy S, Kumar R, Monette M, Stronks HJ, Hume A & Simpson AJ Comprehensive multiphase NMR spectroscopy: basic experimental approaches to differentiate phases in heterogeneous samples. *J Magn Reson* 217, 61–76 (2012). [PubMed: 22425441]
111. Simpson AJ, Courtier-Murias D, Longstaffe JG, Masoom H, Soong R, Lam L, Sutrisno A, Farooq H, Simpson MJ, Maas WE, Fey M, Andrew B, Struppe J, Hutchins H, Krishnamurthy S, Kumar R, Monette M & Stronks HJ *Environmental Comprehensive Multiphase NMR*. *eMagRes*, 399–414 (2013).
112. Ardenkjaer-Larsen JH, Fridlund B, Gram A, Hansson G, Hansson L, Lerche MH, Servin R, Thaning M & Golman K Increase in signal-to-noise ratio of > 10,000 times in liquid-state NMR. *Proc Natl Acad Sci U S A* 100, 10158–63 (2003). [PubMed: 12930897]
113. Kim Y & Hilty C Affinity screening using competitive binding with fluorine-19 hyperpolarized ligands. *Angew Chem Int Ed Engl* 54, 4941–4 (2015). [PubMed: 25703090]
114. Golman K, Ardenkjaer-Larsen JH, Petersson JS, Mansson S & Leunbach I Molecular imaging with endogenous substances. *Proc Natl Acad Sci U S A* 100, 10435–9 (2003). [PubMed: 12930896]
115. Lu M, Wang M, Sergeyev IV, Quinn CM, Struppe J, Rosay M, Maas W, Gronenborn AM & Polenova T (19)F Dynamic Nuclear Polarization at Fast Magic Angle Spinning for NMR of HIV-1 Capsid Protein Assemblies. *J Am Chem Soc* 141, 5681–5691 (2019). [PubMed: 30871317]

116. Franke B, Opitz C, Isogai S, Grahl A, Delgado L, Gossert AD & Grzesiek S Production of isotope-labeled proteins in insect cells for NMR. *J Biomol NMR* 71, 173–184 (2018). [PubMed: 29687312]
117. Bai J, Wang J, Ravula T, Im SC, Anantharamaiah GM, Waskell L & Ramamoorthy A Expression, purification, and functional reconstitution of (19)F-labeled cytochrome b5 in peptide nanodiscs for NMR studies. *Biochim Biophys Acta Biomembr* 1862, 183194 (2020). [PubMed: 31953231]
118. Nogales E The development of cryo-EM into a mainstream structural biology technique. *Nat Methods* 13, 24–7 (2016). [PubMed: 27110629]
119. Barbieri L, Luchinat E & Banci L Characterization of proteins by in-cell NMR spectroscopy in cultured mammalian cells. *Nat Protoc* 11, 1101–11 (2016). [PubMed: 27196722]
120. Wilton DJ, Tunncliffe RB, Kamatari YO, Akasaka K & Williamson MP Pressure-induced changes in the solution structure of the GB1 domain of protein G. *Proteins* 71, 1432–40 (2008). [PubMed: 18076052]
121. Kreuz C, Nußbaumer F, Plangger R, Roeck M (2020) Aromatic ¹⁹F-¹³C TROSY - [¹⁹F, ¹³C] pyrimidine labeling for NMR spectroscopy of RNA. *Angew Chem Int Ed Engl.* 10.1002/anie.202006577

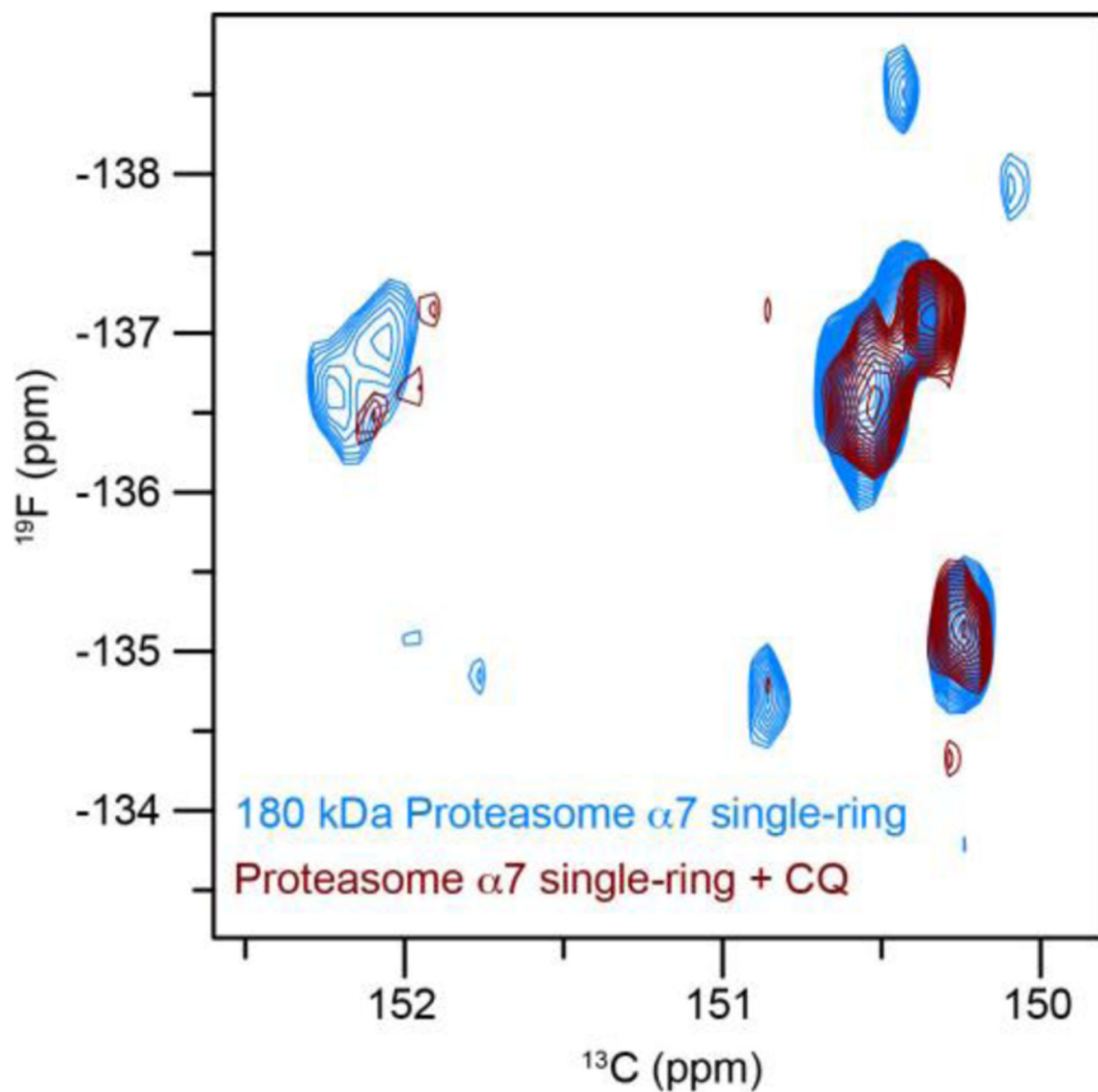


Fig. 1. The 180-kDa $\alpha 7$ single-ring of the 20S proteasome CP from *T. acidophilum* interacts with the antimalaria drug chloroquine (CQ). An overlay of ^{19}F - ^{13}C TROSYs of 1mM apo proteasome $\alpha 7$ single-ring in absence (blue) and in presence of 2 mM CQ is shown (brown). Both experiments were recorded at 45 °C

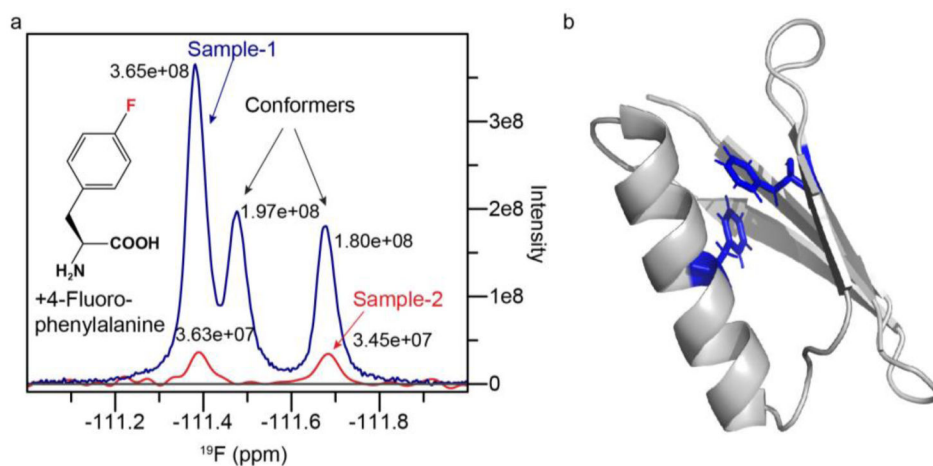


Fig. 2. 4-fluorophenylalanine replaces phenylalanine but not tyrosine. (a) 1D ^{19}F NMR spectra of GB1 grown with 4-fluorophenylalanine as the source of phenylalanine (blue, sample-1) and tyrosine (red, sample-2), respectively. One of the two 4-fluorophenylalanine signals in the spectrum of sample-1 is split into two resonances of similar height, indicating slow exchange on the NMR timescale. The two resonances in the spectrum of sample-2 appear to result from 4-fluorophenylalanine incorporation into phenylalanine positions and not tyrosine. Peak heights are reported next to the corresponding peak positions. (b) The two phenylalanines in the GB1 sequence are highlighted in blue on a solution structure of GB1¹²⁰ (PDB ID: 2j52).

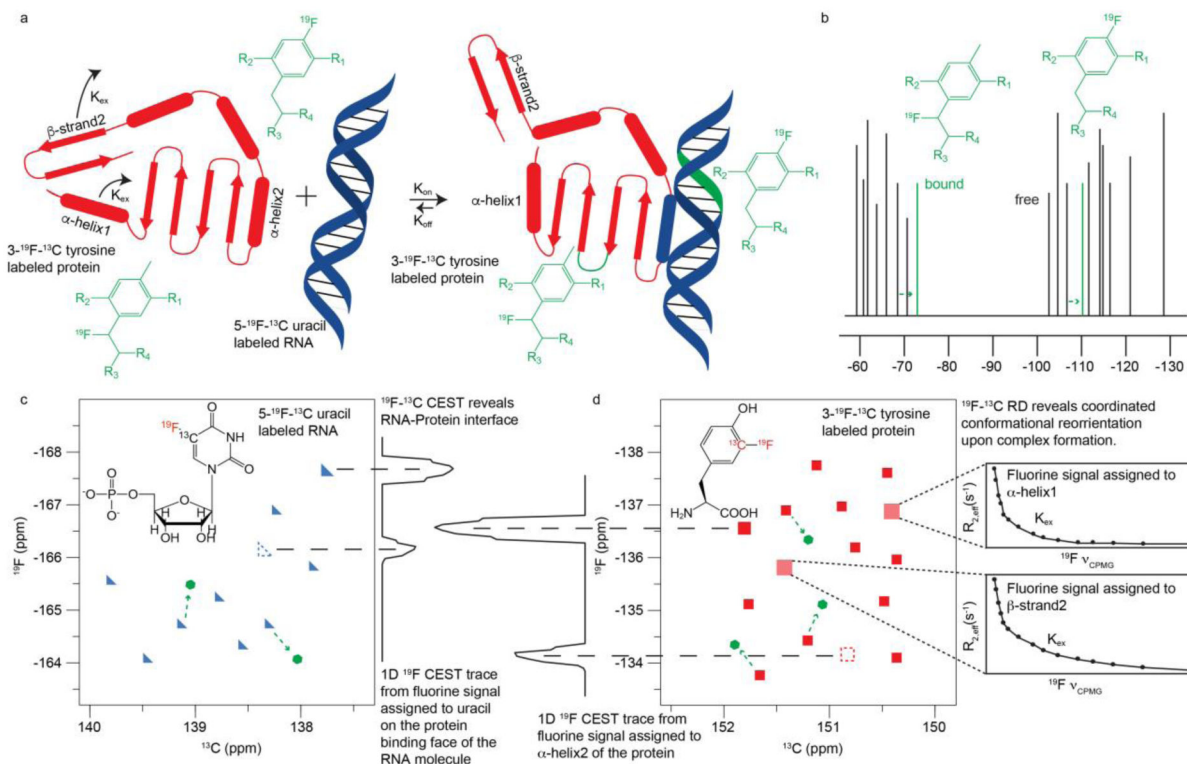
**Fig. 3.**

Illustration of fluorine systems NMR. (a) Schematic of complex formation between fluorine substituted small molecules, a 3-¹⁹F-¹³C-tyrosine labeled protein and a 5-¹⁹F-¹³C-uracil labeled RNA molecule. (b) Hypothetical 1D spectra of a pool of fluorine substituted small molecules are shown in absence (black) and in presence (green) of binding partners. Resonance frequencies of two molecules shift as a consequence of binding to RNA or protein. (c) Schematic of a ¹⁹F-¹³C TROSY of the 5-¹⁹F-¹³C labeled uracil. 2D resonance frequencies are represented as blue triangles and arrows with dotted lines connect ligand free RNA resonances to small molecule bound frequencies (green hexagons). A broader triangle represents a line broadened resonance frequency and is correlated to its invisible protein-bound counterpart (dotted lines) with a 2D ¹⁹F-¹³C CEST experiment. In this experiment, the large dip (inverted peak) corresponds to saturation at the resonance frequency of the ground (free) state and the smaller dip corresponds to saturation at the resonance frequency of the invisible (bound) state. (d) Schematic of a ¹⁹F-¹³C TROSY of the 3-¹⁹F-¹³C tyrosine labeled protein. Dotted lines with arrows connect the free 2D resonance frequencies (red squares) to the small molecule bound frequencies (green hexagons). A 2D ¹⁹F-¹³C CEST experiment correlates the line broadened free and invisible bound resonances (dotted lines) involved in RNA binding. Broad light red rectangles represent line broadened cross-peaks due to microsecond timescale conformational exchange. The kinetics of the conformational exchange and the resonance frequencies corresponding to the invisible state are detected with 2D ¹⁹F-¹³C RD experiments.

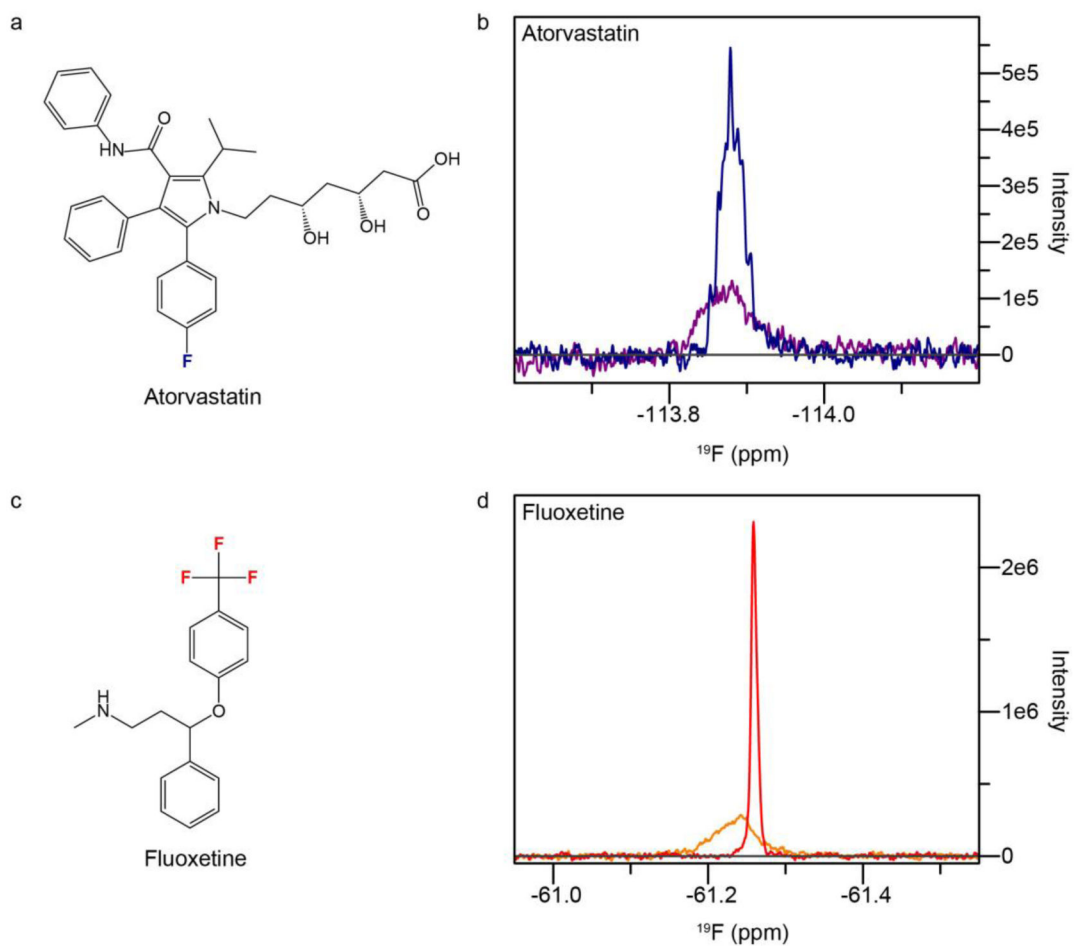
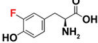
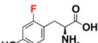
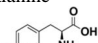
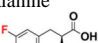
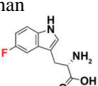
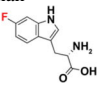


Fig. 4. Fluorine NMR of atorvastatin and fluoxetine in DMEM. (a) Schematic representation of atorvastatin (Lipitor) and (b) 1D fluorine NMR spectra of atorvastatin in absence (blue) and in presence of 10% FBS (purple), respectively. (c) Schematic representation of fluoxetine (Prozac) and (d) 1D fluorine NMR spectra of fluoxetine in absence (red) and in presence of 10% FBS (orange), respectively.

Table 1

Fluorine chemical shifts of fluorine substituted aromatic amino acids in aqueous solution, as reported by Dürr et al.⁷¹ The chemical shift corresponding to the L-form of amino acids is shown where optically pure amino acids were used.

Fluorine substituted aromatic amino acid	Isotropic chemical shift (ppm)
3-fluorotyrosine 	-136.70
2-fluorotyrosine* 	-118
4-fluorophenylalanine 	-115.76
3-fluorophenylalanine 	-113.33
5-fluorotryptophan 	-124.91
6-fluorotryptophan 	-122.18

* An approximate value for 2-fluorotyrosine was obtained from Ycas et al.⁷³.